

# In Vitro Nimesulide Absorption from Different Formulations

F. MERIANI,<sup>1</sup> N. COCEANI,<sup>2</sup> C. SIROTTI,<sup>2</sup> D. VOINOVICH,<sup>3</sup> M. GRASSI<sup>2,4</sup>

<sup>1</sup>Materials Engineering Department DIMCA, University of Trieste, Piazzale Europa 1, I-34127, Trieste, Italy

<sup>2</sup>EURAND S.p.A., Research Department, Via del Follatoio 12, I-34148, Trieste, Italy

<sup>3</sup>Department of Pharmaceutical Sciences, University of Trieste, Piazzale Europa 1, I-34127, Trieste, Italy

<sup>4</sup>Department of Chemical Engineering DICAMP, University of Trieste, Piazzale Europa 1, I-34127, Trieste, Italy

Received 13 June 2003; revised 19 August 2003; accepted 25 August 2003

**ABSTRACT:** In light of improving the bioavailability of poorly water-soluble drugs, this work focused on the comparison among different nimesulide formulations resorting to *in vitro* absorption experiments through everted rat intestine. The performance of a nimesulide ethanol–triacetin solution, an activated system made up by cogrinding nimesulide/polyvinylpyrrolidone and simple solid nimesulide were compared with that of a reference nimesulide solution. Although ethanol–triacetin solution showed a better performance than the solid nimesulide because wettability problems connected with nimesulide were completely zeroed, the activated system showed a better performance than the reference solution one. This was due to the fact that the activated system allowed to overcome both the wettability and solubility problems connected with nimesulide. Moreover, as proved by intestinal pictures taken before and after permeation experiments, we observed the adhesion of polymeric particles to intestinal villi, this giving origin to a thin layer, surrounding the intestine, characterized by a nimesulide concentration higher than that in the release environment bulk. A proper mathematical model, based on Fick's second law, was developed to model drug absorption in the case of solution and activated system. In this manner, we could calculate nimesulide permeability through the intestinal wall, and we could better define the nature of the above-mentioned thin layer surrounding the intestine. Finally, the mathematical model was used to verify the theoretical correctness of the widely employed technique consisting in data correction for dilution when sample withdrawal and replacement were needed to measure drug concentration in the receiver environment. © 2004 Wiley-Liss, Inc. and the American Pharmacists Association *J Pharm Sci* 93:540–552, 2004

**Keywords:** intestine permeability; modeling; poorly water-soluble drugs; drug activation; cogrinding

## INTRODUCTION

Oral dosage form represents the most common route for drug administration into the human body because it leads to a better patient compliance and it is very versatile for what concerns

dosing conditions.<sup>1,2</sup> Unfortunately, however, this strategy fails when dealing with low bioavailable drugs like those belonging to the widely employed anti-inflammatory class.<sup>3</sup> Although bioavailability, defined as the rate and extent to which the active drug is absorbed from a pharmaceutical form and becomes available at the site of drug action,<sup>4</sup> depends on several factors, usually, drug solubility in an aqueous environment and drug permeability through lipophilic membranes play the role of key parameters.<sup>2</sup> In fact, only solubilized molecules can be absorbed by the

---

Correspondence to: M. Grassi (Telephone: 0039 040 8992423; Fax: 0039 040 8992243; E-mail: mario.grassi@eurand.it)

*Journal of Pharmaceutical Sciences*, Vol. 93, 540–552 (2004)  
© 2004 Wiley-Liss, Inc. and the American Pharmacists Association

cellular membranes to subsequently reach the site of drug action (vascular system for instance). According to the high or low values assumed by these parameters, drugs can be divided in four different classes,<sup>5</sup> and a drug can be defined bioavailable if it belongs to the fourth class (high solubility and permeability).

Many different techniques are commonly used to improve the bioavailability of poorly water-soluble but permeable drugs (second class<sup>5</sup>). Apart from the mechanochemical technique, used in this work and later on widely discussed, we can mention drug conglobation inside the lipidic matrix of nano- or microspheres,<sup>6</sup> or drug solubilization in the dispersed lipophilic phase of an O/W emulsion or microemulsion, thus increasing the total amount of drug contained in a mainly aqueous environment.<sup>7-10</sup> A similar task can be achieved using cyclodextrins, cup-like amphiphile macromolecules (lipophile inside and hydrophile outside), which create a complex with the lipophilic drug.<sup>11</sup> By means of solvent swelling and mechanochemical activation it is possible to load a drug into a polymeric carrier in a nanocrystalline or amorphous state, thus considerably increasing its bioavailability.<sup>12,13</sup> Indeed, the interesting aspect of drug nanocrystals and amorphous state relies on the fact that, in these conditions, drug-measured solubility (not the true thermodynamic solubility corresponding to the concentration detectable in a drug solution in equilibrium with a drug crystal of infinite dimensions<sup>14,15</sup>) in hydrophilic fluids is usually much higher than that of the crystalline form,<sup>16,17</sup> so that drug dissolution rate is considerably increased.<sup>12</sup> As both nanocrystals and amorphous drug are not stable and they tend to recrystallize into the more thermodynamically stable macrocrystal size,<sup>14</sup> the polymer, incorporating the drug inside its three-dimensional network, serves as stabilizing agent hindering macrocrystals formation. This action is due to the chemical and physical drug/polymer interactions and to the physical presence of the polymeric chains as macrocrystals that can form on the condition that network meshes be sufficiently wide.<sup>12</sup> Cogrounding has the considerable advantage of not requiring the use of solvents whose elimination from the final formulation can often represent a very expensive and delicate stage. Moreover, the activated system can be administered in the form of tablets or capsules, as both formulations do not modify the "activated" status, and any formulation that does not require the use of solvents or high temperature can in principle be

considered. The use of a particular formulation is essentially related to the desired site of action as one might want to have the release in the intestine instead of in the stomach. Accordingly, in this case, a gastroresistant device should be used to encapsulate the activated system.

Drug bioavailability, in the case of oral administration, is also strongly affected by intestinal permeability. Therefore, drug permeation studies result of paramount importance for the development of those strategies aimed to improve drug absorption, and the necessity of understanding the basic mechanisms ruling the drug transfer through the intestinal epithelium arises.<sup>18</sup> It was demonstrated<sup>19</sup> that *in vivo* drug permeation through the intestinal mucosa mainly takes place according to a passive diffusive mechanism whose rate determining step is represented by the cellular membrane crossing, while a little effect would be exerted by the aqueous stagnant layer arising at the intestinal wall.<sup>19</sup> Although it is usually affirmed that lipophilic drugs follow a transcellular pathway in their intestinal membrane crossing, while hydrophilic ones undertake a paracellular pathway (they would diffuse through the water filling the intercellular voids), today the transcellular way is thought to be the main transport mechanism, both in rats and in human beings, regardless the drug physicochemical properties.<sup>20-24</sup> Although *in vivo* tests undoubtedly represent the most reliable techniques to study intestine drug permeability, and some preliminary information can be obtained resorting to theoretical predictive approaches,<sup>25,26</sup> the increasing demand for a rapid bioavailability estimation and the costs connected to *in vivo* test led us to consider a simplified approach represented by the everted rat intestine<sup>27-30</sup> technique. Indeed, we found that this approach is very useful for what concerns bioavailability estimation when the rate determining step of the drug absorption process is represented by drug solubility. Although this is surely a partial vision of the whole problem (drug absorption), it is exactly what we are interested in checking, as the activated system can act only on drug solubility, being all other factors (drug permeability among them) independent from our drug activation.

The aim of this work was to compare the performance of different nimesulide formulations with respect to that of a reference, represented by a nimesulide aqueous solution. In particular, we considered solid nimesulide in powder form, an activated system (made up by cogrounding

polyvinylpyrrolidone and nimesulide) and a solution of ethanol/triacetin in which the drug was solubilized (this formulation was previously characterized from the liquid/liquid interface properties point of view<sup>31</sup>). These systems were chosen as they should clarify the relative importance of solubility and wettability problems affecting a delivery system containing a poorly soluble and wettable drug like nimesulide. Solid nimesulide in powder form was chosen, as it is the worst system for nimesulide delivery being affected by both wettability and solubility problems, while the activated system should overcome these drawbacks. Finally, the ethanol/triacetin solution should be affected only by solubility problems as discussed later.

To better understand our findings, the permeation results referring to the activated system and drug solution were studied, resorting to a mathematical model based on Fick's second law assuming that nimesulide transport across intestinal wall occurs according to a pure diffusive mechanism.

Nimesulide was considered as model drug as it is a typical NSAID (Nonsteroidal Anti-Inflammatory Drug), characterized by a low bioavailability.<sup>32,33</sup>

## MATERIALS AND METHODS

Intestine permeation experiments were performed using as donor and receiver phases a Krebs Ringer modified buffer (pH = 7.4; 37°C), able to maintain the homeostasis of the intestine cells.<sup>34</sup> Nimesulide (HELSINN, Pambio Noranco, CH; supplied in solid powder form; anti-inflammatory action) and phenol red (Sigma Chemical, Steinheim, D) were chosen as the model drug and marker, respectively, for their wide use in this field.<sup>20,35,36</sup>

Nimesulide solubility in buffer solution was measured by adding small drug amounts, under gentle stirring in thermostatic conditions (37°C), in a known solvent volume until the attainment of a permanently turbid system. The system was left to rest overnight, then concentration was measured by means of a UV spectrophotometer (Lambda 6/PECSS System, Perkin-Elmer Corp., Norwalk, CT, wavelength 393.4 nm). The resulting solubility was  $160 \pm 5 \mu\text{g}/\text{cm}^3$ .

To measure nimesulide permeability through the rat intestine and to have a reference permeation curve, a nimesulide/buffer pH 7.4 solution (37°C) ( $100 \mu\text{g}/\text{cm}^3$ ) was realized by dispersing

a proper drug amount in a well-stirred buffer environment. The system was left under mixing conditions overnight to finally get a clear yellow solution.

Ethanol (Merck, Germany) and triacetin (Merck, Germany), mixed in a ratio 1:3 (w/w), gave origin to a solution where nimesulide was added to obtain a concentration equal to  $70 \text{ mg}/\text{cm}^3$  (37°C).

Finally, the activated system was prepared by cogrinding for 2 h in a planetary mill (Pulverisette 7, Fritsch GmbH, D), at 350 rpm, crosslinked polyvinylpyrrolidone (PVP-clm, Basf, Germany), and nimesulide using a drug/polymer ratio equal to 1:3 (w/w). The two mill vials, made up by agate, contained seven agate balls (1-cm diameter) plus 0.375 g nimesulide and 1.125 g PVP-clm each. We choose a planetary mill as its dynamic behavior, and thus the energy transfer to coground materials, is well understood.<sup>37</sup> The activated system was then characterized by means of a X-rays diffractometer equipped with a Cu K $\alpha$  source (40 kV, 20 mA) (Stoe 500, Siemens, Germany) and differential scanning calorimetry analysis (DSC 7, Perkin-Elmer Corp., Norwalk, CT). The comparison among the X-rays pattern of the coground material, pure nimesulide and the simple nimesulide/PVP-clm physical mixture (ratio 1:3, w/w), allowed to conclude that no polymorphic transformation occurred during the cogrinding process. DSC 7 analyses revealed<sup>38,39</sup> that after 2 h cogrinding the 75% of the original crystalline drug was transformed into amorphous phase while the remaining 25% was transformed into a nanocrystalline phase. Indeed, while original nimesulide melting temperature was 148.7°C (melting enthalpy  $\Delta H = 108.7 \text{ J/g}$ ), in the activated system we measured a nimesulide melting temperature equal to 118°C (melting enthalpy  $\Delta H = 5.1 \text{ J/g}$ ). Moreover, no thermal events took place at 148.7°C. As it is well known that, in the absence of polymorphic phase transformations (as previously demonstrated by the X-rays analysis), melting temperature reduction is due to drug crystal size reduction to the nanoscale,<sup>17,40</sup> we could affirm that the residual crystallinity detected was only due to nimesulide nanocrystals.

The determination of nimesulide dissolution constant  $k_d$  (it comprehends any mass transfer resistance from the activated system) was performed by monitoring the drug concentration increase when 400 mg of activated system were put in the donor environment in the absence of intestines. The use of a fiber optic apparatus (ZEISS,

Germany), connected to a spectrophotometer (ZEISS, Germany, wavelength 393.4 nm), allowed the determination of nimesulide concentration without perturbing the donor environment. Moreover, this methodology allowed to easily overcome the problem connected to drug concentration measurement in the presence of a solid particle dispersion. Indeed, while the maximum nimesulide absorption in aqueous solution occurred at 393.4 nm, the scattering effect due to solid particles uniformly occurred at every wavelength. Accordingly, the real absorbance related to nimesulide concentration was the difference between the measured absorbance at 393.4 nm and that measured at 500 nm (at this wavelength we were sure that nimesulide did not absorb). The determination of particles mean radius  $R_m$  was achieved by determining the activated system particle size distribution in the swollen state by means of a laser light scattering (Malvern, U.K.).  $R_m$  was calculated according to the following weighted sum:

$$R_m = \frac{\int_{r_{\min}}^{r_{\max}} r f(r) dr}{\int_{r_{\min}}^{r_{\max}} f(r) dr} = 4 \mu\text{m} \quad (1)$$

where  $r$  is particle radius,  $f(r)$  is particle distribution frequency while  $r_{\min}$  and  $r_{\max}$  are, respectively, the distribution minimum and maximum radius.

To compare the three formulations considered (solid nimesulide in powder form, nimesulide–ethanol–triacetin solution and activated system) and our reference (nimesulide solution), four different kinds of experimental tests were performed. In the reference case, the donor environment  $V_d$  was filled by 1000 cm<sup>3</sup> buffer pH = 7.4 solution (37°C) characterized by a nimesulide concentration equal to 100 µg/cm<sup>3</sup>. Uniformity conditions in the donor environment were ensured by means of an impeller (rotational speed 70 rpm; see Fig. 1). In the remaining situations (solid nimesulide in powder form, nimesulide–ethanol–triacetin and activated system) a proper amount of formulation (100 mg for the solid nimesulide in powder form, 1.43 cm<sup>3</sup> for the nimesulide–ethanol–triacetin solution, 400 mg for the activated system) was added, at time zero, to the donor environment (in this manner, the same nimesulide amount was always added to the release environment). Again, uniformity conditions in the donor environment were ensured by

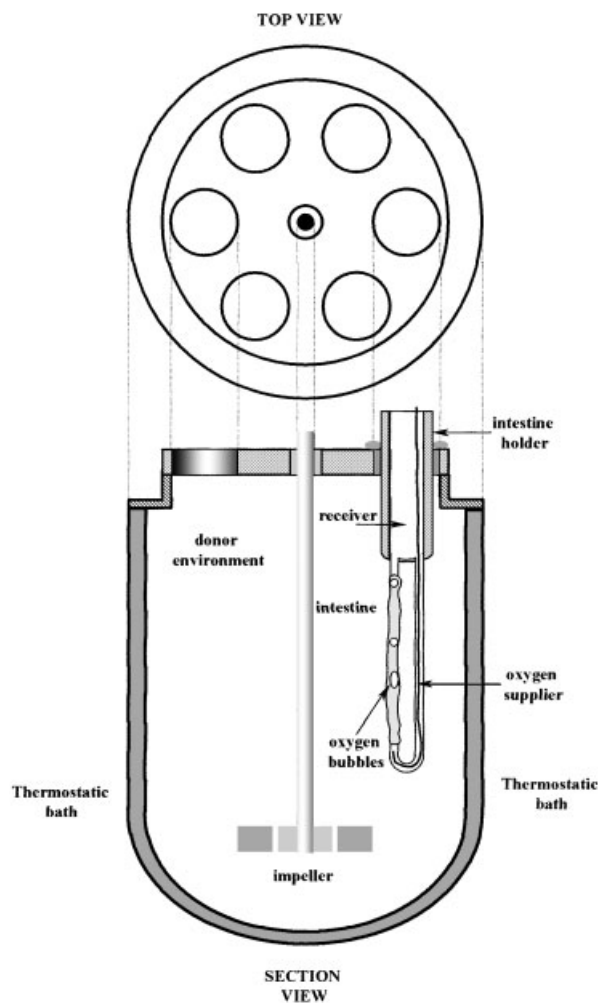


**Figure 1.** Experimental setup. Each intestine holder is a cylindrical vessel connected to a “U” capillary whose left portion is represented by intestine. Intestine holders are placed on a holding plate.

means of an impeller. Regardless the formulation considered, four intestine sections were hosted in the donor environment.

Male Wistar rats (Centro servizi di Ateneo, Settore Stabulario e Sperimentazione animale, Trieste University, Italy) weighing approximately 250 g were fasted for 12 h (water ad libitum), then sacrificed by CO<sub>2</sub>. Small intestine (duodenum, jejunum, and ileum) was removed, separated from the mesentery, rinsed with the buffer using a 10-mL syringe, then cut in four different sections. Each section was everted on a Teflon rod, and fixed on its location by means of surgical thread. The experimental set up is illustrated in Figure 1. Intestine holder was a cylindrical glass vessel connected to a “U” glass capillary whose left portion



was represented by intestine. A symmetrical intestine holder disposition on the holding plate was needed to avoid preferential fluxes inside the donor due to stirring. Intestine holders volume (four in our case), filled by buffer, represented the receiver environment ( $V_r = 4 \cdot 12 \text{ cm}^3 = 48 \text{ cm}^3$ ). Both receiver and donor phases were continuously oxygenated (95%  $\text{O}_2$ , 5%  $\text{CO}_2$ ), to keep the intestine cells alive during the experiment. Moreover, oxygen bubbles ensured receiver volume homogeneity.

At the beginning of the permeation test ( $t = 0$ ) the formulation was added to the donor environment, and every 12 min 4  $\text{cm}^3$  of the receiver phase were sampled from each intestine holder and replaced with pure buffer, for a total time of 60 min. Nimesulide concentration  $C_r$  in each of the four liquid phases sampled was measured by UV spectrophotometer (Lambda 6/PECSS System, Perkin-Elmer Corp., Norwalk, CT, wavelength 393.4 nm). As each experimental test was led on three different rats, drug concentration at each time was the mean of 12 experimental data.

For a correct evaluation of the experimental data, it was necessary to verify the good homeostasis of the intestine cells during the experiment. This is associated to phenol red (marker) permeability values between  $6 \cdot 10^{-4} \text{ cm/min}$  and  $9 \cdot 10^{-4} \text{ cm/min}$ , as higher values are symptom of progressive cells dying.<sup>34</sup> As we measured (according to the procedure described later on) a phenol red permeability across the intestinal membrane equal to  $7.8 \cdot 10^{-4} \text{ cm/min}$ , we could affirm that the integrity of the system was ensured during the 60 min of the experiment. A blank permeation test (no nimesulide in the donor phase) was performed, to verify that the intestinal secretions did not interfere with the absorption process.<sup>18</sup> Approval of this study was given by the Italian Ministry of Health (D. LVO 116/92) in accordance with the "Principle of Laboratory Animal Care."

## THEORETICAL

To model nimesulide accumulation inside the receiver environment (namely, intestine holders volume), it was necessary to take into account both drug release from the chosen formulation and the subsequent permeation process occurring through the intestinal wall. Due to the low practical interest, the mathematical description of nimesulide release and permeation relative to the solid nimesulide in powder form (at time zero

a known amount of pure drug was put in the buffered donor environment) was not considered. Similarly, the mathematical analysis of nimesulide release and permeation relative to the nimesulide-ethanol-triacetin system (at time zero a known volume of nimesulide-ethanol-triacetin solution was put in the buffered donor environment) was not matched due to the complexity and the uncertainty connected to the description of this particular kind of drug release, as discussed later on. Accordingly, attention was focussed on the solution case (at time zero the buffered donor environment was a nimesulide solution of known concentration) and on the activated system case (at time zero a known amount of activated system was put in the buffered donor environment). From the modelling point of view, it will be shown in the following that the solution case can be considered as the particular case of the activated system case where drug release from particles is instantaneous.

Although drug release from an ensemble of drug-loaded polymeric particles is a complex phenomenon,<sup>12</sup> for the purposes of this work we could assume that particle swelling is instantaneous, that we were dealing with a monodisperse particles system (mean radius  $R_m$ ) and that drug release was essentially ruled by particles surface area, while drug diffusion through the polymeric network played a minor role. Indeed, loading technique based on cogrinding implies the drug mainly occupying the outer part of the particles as proved by SEM pictures evidencing many drug nanocrystals emerging from particles surface. On the contrary, in the case of activated systems loaded by solvent swelling,<sup>12</sup> no nanocrystal are detectable as the drug is present in the inner particles region. Moreover, intestine was assumed to be a perfect cylinder (see Fig. 2), characterized only by its length  $L$  and by its internal and external

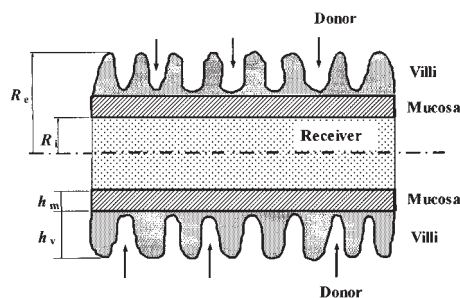


**Figure 2.** Schematic representation of a rat intestine portion.

radius  $R_i$  and  $R_e$ , respectively. In so doing, the real physical frame was considerably simplified as we neglected the presence of villi and microvilli that greatly increase permeation area. Accordingly, the real drug diffusion coefficient inside the intestinal wall will be much smaller (one or two orders of magnitude) than the apparent one determined in this study. Indeed, assuming that  $D^*A^*\nabla C = D_{\text{REAL}}^*A_{\text{REAL}}^*\nabla C$ , (where  $D_{\text{REAL}}$  and  $A_{\text{REAL}}$  are, respectively, the real drug diffusion coefficient and luminal surface,  $D$  and  $A$  are, respectively, the apparent diffusion coefficient and the cylinder surface, while  $\nabla C$  is the concentration gradient), we can say that the ratio  $D_{\text{REAL}}/D$  is equal to  $A/A_{\text{REAL}}$ , which is much smaller than 1. Of course, the difference existing between  $D$  and  $D_{\text{REAL}}$  was not a serious drawback, as we were mainly interested in describing the permeation process (evaluation of drug amount crossing the intestinal membrane), rather than measuring the real drug diffusion value.

Considering the intestine as a uniform membrane, drug permeation could be described, in cylindrical coordinates, according to Fick's second law:

$$\frac{\partial C(r)}{\partial t} = \frac{1}{r} \frac{\partial}{\partial r} \left( D \frac{\partial C(r)}{\partial r} \right) \quad (2)$$

where  $r$  was the generic cylinder radius between  $R_i$  and  $R_e$ ,  $C(r)$  was nimesulide concentration at radius  $r$ ,  $t$  was time, and  $D$  was nimesulide apparent diffusion coefficient in the intestinal membrane. Drug concentration  $C_p$  in the particles and in the donor environment  $C_d$  were determined by the following system of equations:

$$\frac{dC_p}{dt} = -\frac{N_p 4\pi R_m^2 k_d}{V_p} (C_p - C_d) \quad (3)$$

$$\frac{dC_d}{dt} = \frac{N_p 4\pi R_m^2 k_d}{V_d} (C_p - C_d) - 2\pi R_e L D \frac{\partial C(r)}{\partial r} \Big|_{r=R_e} \quad (4)$$

where  $N_p$  and  $V_p$  were, respectively, particles number and volume,  $V_d$  was the donor environment volume, while  $k_d$  was the dissolution constant accounting for any mass transfer resistance occurring in drug release from particles. Remembering that for a monodispersed particles system the following relation holds:

$$N_p = \frac{V_p}{4\pi R_m^3/3} \quad (5)$$

eqs. 2 and 3 could be more conveniently rewritten as follows:

$$\frac{dC_p}{dt} = -\frac{3k_d}{R_m} (C_p - C_d) \quad (3')$$

$$\frac{dC_d}{dt} = \frac{3V_p k_d}{R_m V_d} (C_p - C_d) - 2\pi R_e L D \frac{\partial C(r)}{\partial r} \Big|_{r=R_e} \quad (4')$$

Equations 2–4 had to accomplish the following initial and boundary conditions:

*initial conditions:*

$$C_r(t = 0) = C_{r0} = 0 \quad (6)$$

$$C(r) = 0 \quad R_i < r < R_e \quad (7)$$

$$C_p(t = 0) = C_{p0} \quad (8)$$

$$C_d(t = 0) = C_{d0} \quad (9)$$

*boundary conditions:*

$$C(r = R_i) = C_r K_{pr} C(r = R_e) = C_d K_{pd} \quad (10)$$

$$M_0 = V_d C_d + V_r C_r + V_p C_p + \int_{R_i}^{R_e} C(r) 2\pi L r dr \quad (11)$$

where  $V_r$  and  $C_r$  were, respectively, nimesulide concentration and volume of the receiver environment,  $C_{p0}$ ,  $C_{d0}$ , and  $C_{r0}$  represented, respectively, initial drug concentration in the particles, in the donor environment and in the receiver environment,  $M_0$  was total drug amount present in system (donor and receiver environment plus intestine),  $K_{pr}$  and  $K_{pd}$  were, respectively, the intestine/receiver and intestine/donor partition coefficient.

Equation 3 imposed that drug release from the particles was ruled by particles surface area, dissolution constant, and concentration gradient between particles and donor environment. Equation 4 accounted for the fact that drug concentration variation in the donor environment resulted from the algebraic sum of the positive drug flux coming from the particles and the negative drug flux going in the receiver environment through the intestinal wall. Equations 6–7 stated that, at the beginning of the experiment, the intestine and the receiver environment were drug free while eqs. 8–9 stated that drug could be present in the particles and/or in the donor environment. Equation 10 imposed the partitioning conditions at the intestine/receiver and intestine/donor interface, while eq. 11 was an overall mass balance performed on the particles, donor and receiver

environments, and intestinal membrane, allowing the determination of  $C_r$ .

Due to the simultaneous presence of ordinary and partial differential equations, beside the overall mass balance condition expressed by eq. 11, model solution could be achieved only by means of numerical techniques. In particular, eq. 2 was solved according to the control volume method,<sup>41</sup> while eqs. 3–4 were solved according to the fifth order Runge-Kutta method with adaptive step-size.<sup>42</sup> The particular nature of the proposed model required, step by step, to iteratively solve the system made up by eqs. 2–4. Indeed, at each time step, eqs. 3 and 4 were solved according to the old drug concentration profile inside the intestinal wall. Then, on the basis of the new  $C_p$  and  $C_d$  values, eq. 2 was solved. If the new  $C(r=R_e)$  value differed from its old value more than a fixed tolerance, eqs. 3–4 were solved again assuming for  $C(r=R_e)$  the mean calculated from the actual and the old value. This process proceeded until convergence. To ensure a satisfactory solution accuracy, we subdivided the intestinal wall in 20 parts and we assumed the computational time step  $dt = 0.025$  min.

It is interesting noticing that when  $k_d$  became bigger and bigger, we approached to the solution condition, namely the situation in which the donor environment was a drug solution from the beginning of the experiment. In this particular situation, eq. 3 (and, thus, the first right-hand term of eq. 4) became meaningless and the model reduced to the solution of eq. 2 with the boundary conditions expressed by eqs. 4, 7–11. Consequently, drug permeability  $P$  through the intestinal membrane<sup>43</sup> could be calculated according to the following equation:

$$P = \frac{DK_p}{h_m + h_v} \quad (12)$$

where  $K_p$  was the partition coefficient,  $h_m$  was the real wall thickness and  $h_v$  the villi layer thickness (see Fig. 2). Considering the villi layer morphology, it was acceptable to consider  $h_m + h_v$  as the effective intestine wall thickness.<sup>27</sup>

When the intestine was not present in the donor environment, the proposed model reduced to the following equations:

$$\begin{aligned} \frac{dC_p}{dt} &= -\frac{3k_d}{R_m}(C_p - C_d) \quad C_p(t=0) \\ &= C_{p0} \quad C_d(t=0) = C_{d0} = 0 \end{aligned} \quad (13)$$

$$C_r = \frac{M_0 - V_p C_p}{V_r} \quad (14)$$

whose analytical solution was:

$$C_p = \left( C_{p0} - \frac{M_0}{V_r + V_p} \right) e^{-\left( \frac{3k_d}{R_m} \frac{V_r + V_p}{V_r} \right) t} + \frac{M_0}{V_r + V_p} \quad (15)$$

## RESULTS AND DISCUSSION

Because of the technique used for the  $C_r$  measurements (sampling and subsequent replacement with pure buffer), experimental data were corrected for dilution according to the following expression:

$$C_{\text{corr}}^i = C_{\text{experim}}^i + \frac{\Delta V}{V_r} \sum_{j=1}^{i-1} C_{\text{experim}}^j \quad (16)$$

where  $C_{\text{corr}}^i$  was the concentration value corrected for dilution,  $C_{\text{experim}}^i$  was the measured value,  $V_r$  was the receiver environment volume, and  $\Delta V$  the sampled volume. Figure 3 shows the nimesulide concentration  $C_r$  variation in the receiver relatively to the formulations considered. Triangles refer to the activated system, squares to the solution, and circles to the triacetin-ethanol system. The data relative to solid nimesulide in powder form were not reported, as the drug presence in the receiver environment was not detectable during the 60 min of the experiment (this was principally due to the low wettability of crystalline nimesulide). It is interesting noticing that the standard error bars indicate a satisfactory reproducibility of the

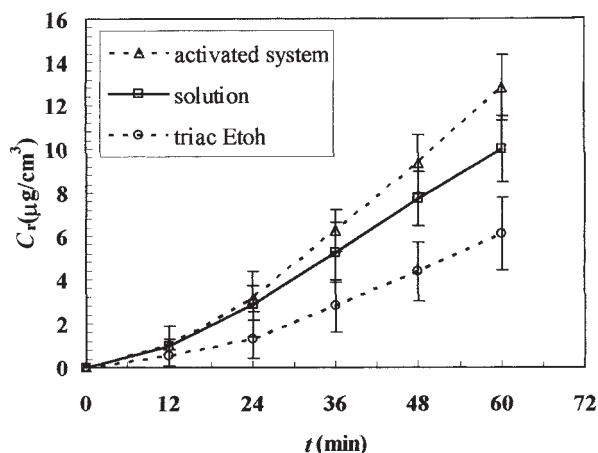


**Figure 3.** Nimesulide absorption curves (concentration in the intestinal lumen  $C_r$  versus time  $t$ ) from the different release systems considered (triangles, activated system; squares, solution; circles Triac-EtOH system). Vertical bars indicate datum standard error.

experimental data (each point is the mean value of 12 measurements).

The triacetin–ethanol–nimesulide system presented a bioavailability increase compared to solid nimesulide in powder form, but not as good as the other formulations considered. The explanation of this behavior could be given on the basis of a qualitative observation about the release mechanism from this formulation. At the beginning of the experiment, the triacetin–ethanol–nimesulide solution volume was broken in several spherical particles due to the donor environment stirring, thus leading to an increase in the interfacial area between the two liquid phases (buffer and oil–alcohol solution). Subsequently, because of the different chemical potential in the two phases, ethanol and triacetin (it has a partial solubility in the buffer phase<sup>31</sup>) started to move into the buffer phase, with a consequent oil phase impoverishment. Both ethanol and triacetin migration was observable, in a qualitative way, in the form of an evident translucent layer surrounding the oil–alcohol drops. These phenomena caused the recrystallization of several nimesulide molecules as proved by drops transparency reduction determined by crystals deposition on the drops surface. As the experiment proceeded, more and more ethanol and triacetin left the drops, so that, after about 10 min, several small sponge-phases mostly composed by nimesulide crystals were formed. Accordingly, drug release was mainly governed by crystals dissolution in the aqueous environment (this phenomenon was heavily affected by drug solubility), although we could not exclude that part of the nimesulide molecules migrated directly in the buffer during sponges formation. Ethanol–triacetin–nimesulide formulation had, then, the advantage of zeroing all the bioavailability problems connected to nimesulide wettability. In this manner, we were experimentally able to split the contribution of wettability and solubility to nimesulide absorption through everted rat intestines. Indeed, for what we said before, the difference existing between the triacetin–ethanol–nimesulide absorption curve (circles, Fig. 3) and the solution one (squares, Fig. 3), was ascribed only to nimesulide crystals dissolution and not to nimesulide crystals wetting. When both solubility and wettability problems occurred (this was the case of solid nimesulide in powder form), the resulting absorption curve did not significantly detach from the abscissa axis of Figure 3.

Interestingly, Figure 3 also shows that the activated system had a better performance than

that of nimesulide solution. This behavior could be explained by the presence of a thin stagnant layer originated by PVP particles aggregation and adhesion on the intestine wall. Due to the presence of mucus, mixing conditions in the layer were vanishing so that drug exchange with the donor environment could take place only according to a diffusive mechanism, being the convective route hindered by mucus viscosity. Consequently, the layer drug concentration could be higher than that in the donor environment and the  $100 \mu\text{g}/\text{cm}^3$  threshold could be easily exceeded. Indeed, the solubility of amorphous or nanocrystalline organic drugs can be higher than that of the same drug in the crystalline form.<sup>12,16,17</sup> The increased concentration gradient across the intestine wall justified our experimental results. Biological and hydrodynamical considerations explained the stagnant layer formation. Indeed, particles adhesion on intestine wall was enhanced by intestinal villi, faced in the donor environment due to the everted configuration adopted, designed to capture solid lipid particles and responsible for a huge and rough intestinal interfacial area. Moreover, the stirring conditions imposed in the donor environment caused a rotational motion forcing polymeric particles against the half part of intestinal wall exposed to fluid stream. On the other intestine side, the formation of vortexes due to a little depression, favored particles stagnation and deposition on the intestinal wall. Picture of the intestinal wall before the permeation experiment (Fig. 4a) and after, in the case of 60-min exposure to solution (Fig. 4b) and to activated system (Fig. 4c) showed the correctness of this physical frame. It can be seen that while at the beginning intestine surface was mainly smooth (Fig. 4a), after exposure to solution (Fig. 4b) it became more irregular due to unavoidable tissues degeneration. Nevertheless, after exposure to activated system (Fig. 4c), we could clearly see the existence of structures (see the white arrow) that we never found in the previous case (Fig. 4b) (this was based on many intestinal pictures and not only on the three here shown). These structures were clusters of polymeric particles and mucus (Fig. 4c). Moreover, a visual inspection of the intestinal wall after a permeation test led in the presence of the activated system, revealed the existence of a yellow viscous layer on the intestine surface (we remember here that nimesulide solution has a yellow color).

The developed mathematical model could, indirectly, supply a further confirmation of what is now affirmed. Indeed, the existence of the



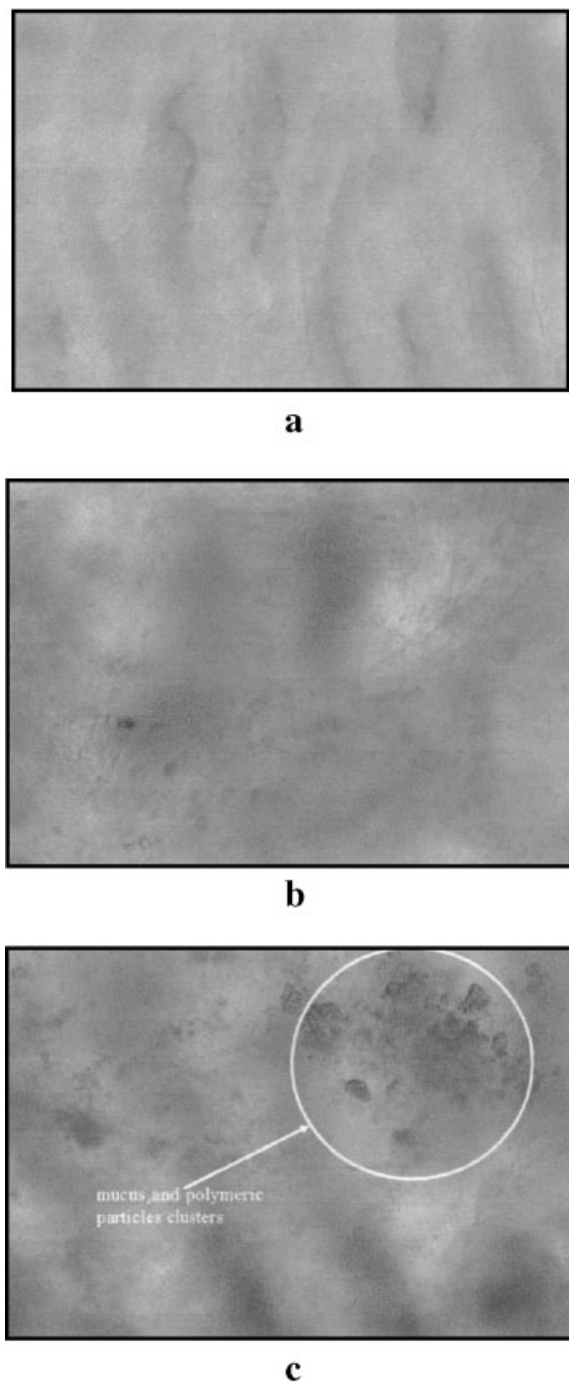


**Figure 4.** Pictures (zoom  $8.5\times$ ) of intestinal surface before the permeation experiment (a), after 60-min exposure to nimesulide solution (b) or after 60-min exposure to activated system dispersion (c). The white arrow indicates the presence of particles and mucus clusters (c).

surrounding layer could be easily considered assuming that the drug partition coefficient (intestine/donor)  $K_{pd}$  was greater than 1. If the model had been able to satisfactorily fit the experimental

data (see triangles in Fig. 3) assuming a reasonable  $K_{pd}$  value (it means not too high), all other parameters values being known and fixed, our hypothesis would have been further supported. At this purpose, it was necessary to preventively measure nimesulide dissolution constant  $k_d$  from the activated system by data fitting according to our model expression relative to intestine absence in the donor environment (eq. 15). Knowing that  $V_d = 1000 \text{ cm}^3$ ,  $V_p = 0.31 \text{ cm}^3$  (it corresponds to 400 mg of activated system),  $C_{p0} = 321 \text{ mg/cm}^3$ ,  $M_0 = 100 \text{ mg}$  and  $R_m = 4 \times 10^{-4} \text{ cm}$ , fitting procedure yielded  $k_d = 8.3 \times 10^{-5} \text{ cm/min}$ . Figure 5 shows good agreement between the model (solid line) and experimental data (open circles) in the initial and final part of the curve, while a clear bias appears in the central part (data overestimation can be mainly due to the hypothesis of an instantaneous drug diffusion, even if the monodisperse hypothesis makes the system different from reality). Nevertheless, we believe that the model was able to catch the essence of the phenomenon under evaluation. Now, knowing that apparent nimesulide diffusion coefficient  $D$  through intestinal wall was  $1 \times 10^{-4} \text{ cm}^2/\text{min}$  (as later on demonstrated), it was possible to perform data fitting knowing that  $V_d = 1000 \text{ cm}^3$ ,  $V_p = 0.31 \text{ cm}^3$  (it corresponds to 400 mg of activated system),  $C_{p0} = 321 \text{ mg/cm}^3$ ,  $M_0 = 100 \text{ mg}$ ,  $R_m = 4 \times 10^{-4} \text{ cm}$ ,  $k_d = 8.3 \times 10^{-5} \text{ cm/min}$ ,  $V_r = 48 \text{ cm}^3$ ,  $L = 36 \text{ cm}$  (sum of four intestine parts),  $R_e = 0.27 \text{ cm}$  and  $R_i = 0.21 \text{ cm}$ . Figure 6 shows that a good agreement between experimental data (triangles) and model best fitting (solid line) is achieved when  $K_{pd} = 1.3$ . The relatively low

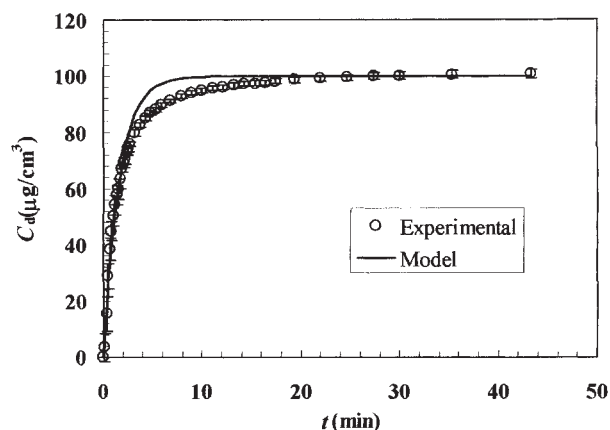


**Figure 5.** Nimesulide concentration increase ( $C_d$ ) when intestine is not present in the donor environment. Circles represent experimental data, while solid line indicates model best fitting (eq. 15) (vertical bars indicate datum standard error).

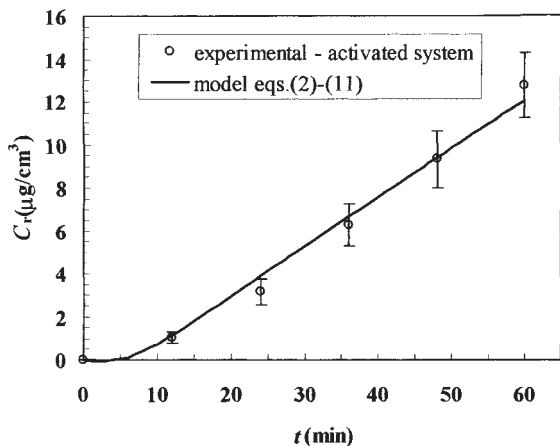


**Figure 6.** Comparison between experimental data (circles) referring to the activated system release and model best fitting (eqs. 2–11) (vertical bars indicate datum standard error).

value assumed by  $K_{pd}$  not only confirmed model reliability, but further supported the hypothesis of the existence of a thin layer surrounding the intestinal wall. Indeed, it was sufficient that drug concentration in the layer was on the average (more correctly,  $K_{pd}$  should be time dependent) 30% higher than that in the bulk. Remembering that layer thickness is very small, a limited amount of activated system was required to support this concentration increase. Accordingly, bulk concentration was not sensibly affected by the presence of the surrounding layer. Ultimately, we could say that the activated system strongly reduced both wettability and solubility problems considerably improving nimesulide bioavailability.

Before determining apparent nimesulide diffusion coefficient  $D$  inside intestine wall (and the relative permeability  $P$ ), some considerations had to be done.  $D$  (and  $P$ ) could be, in principle, obtained by fitting the proposed model (eqs. 2, 4, 7–11; donor environment filled by a nimesulide solution) on the absorption data coming from nimesulide solution (squares in Fig. 3). Nevertheless, a more correct procedure consisted in fitting the model on the raw experimental data, that is, not corrected for dilution. In fact, while eq. 16 took into account the progressive drug mass uptake from the system, it did not account for the variation of the concentration gradient between donor and receiver taking place at each replacement.

The raw data fitting was possible because the model required a numerical solution, whose programming easily allowed the introduction of the

sampling and replacement condition, which means an instantaneous reduction of the receiver concentration at each replacement. To quantify the theoretical error connected with model fitting performed on data corrected for dilution, a dimensionless analysis resulted to be useful (see Fig. 7). Assuming that drug permeability  $P$  was equal to  $5.0 \cdot 10^{-3}$  cm/min, the continuous line depicted in Figure 7 represents the simulated dimensionless concentration profile  $C_r^+$  in the receiver environment as a function of the dimensionless time  $t^+$ , defined as follows:

$$C_r^+ = \frac{C_r}{C_{r\infty}} \quad (17)$$

$$t^+ = \frac{tD}{(R_e - R_i)^2} \quad (18)$$

where  $C_{r\infty}$  was drug concentration in the receiver environment after an infinitely long time. Using the proposed model backwards, it was possible to calculate the simulated concentration values relative to ten different hypothetical permeation experiments, characterized by sampling and replacements equal to 0.1, 0.2, 0.3, 0.4, 0.5, 0.6, 0.7, 0.8, 0.9, and 1 of the receiver volume. These data, corrected according to eq. 16, are shown in Figure 7. It was clear that the larger the volume sampled, the wider the difference existing among the real (solid line) curve and the curves obtained from the experimental data correction according

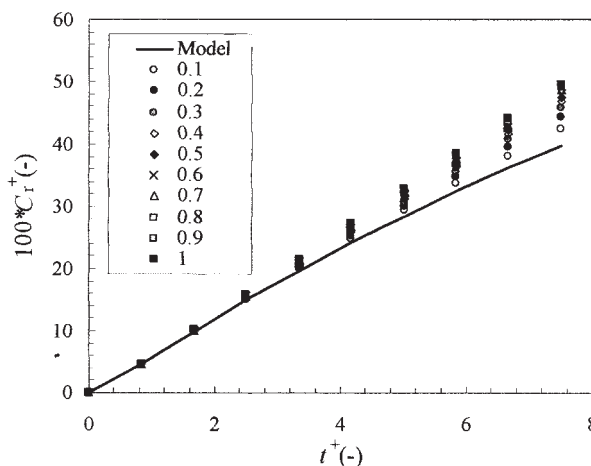


**Figure 7.** Comparison between the theoretical permeation curve (solid line) and the pseudoexperimental data (symbols) obtained after correction for dilution according to eq. 16, for different values of  $V_{ratio}$  (ratio between sampled and receiver volume).

to eq. 16 (symbols). To better quantify this difference, the model was fitted on the pseudo-experimental data shown in Figure 7 and the corresponding permeability values ( $P_{\text{corr}}$ ) were determined. Figure 8 illustrates how the ratio  $P_{\text{corr}}/P$  increases when the ratio between the sampled volume and the receiver volume,  $V_{\text{ratio}}$ , increases. Although Figure 8 was drawn in respect to the usual experimental conditions relative to *in vitro* permeations, the entity of the errors is purely indicative, as it also depends on the number of experimental points considered in the fitting, and on the values assumed by  $C_r^+$  (error entity increases with the sampling number and with  $C_r^+$ ).

According to these considerations, the evaluation of  $D$  (and  $P$ ) was made on not corrected data, as shown in Figure 9. As the model best fitting was able to reproduce experimental data, we could conclude that the physical phenomena characterizing nimesulide permeation through everted rat intestine were properly taken into account. Considering  $K_p = 1$ ,  $R_i = 0.21$  cm,  $h_v + h_m = 0.06$  cm,  $L = 36$  cm,  $C_{d0} = 100$   $\mu\text{g}/\text{cm}^3$ , the fitting of the experimental data yielded  $D = (1.0 \pm 0.2) \cdot 10^{-4}$   $\text{cm}^2/\text{min}$ , and consequently,  $P = (1.7 \pm 0.4) \cdot 10^{-3}$   $\text{cm}/\text{min}$  (the same procedure was used to measure phenol red permeability and we got  $P = 7.8 \cdot 10^{-4}$   $\text{cm}/\text{min}$ ). These values confirmed that nimesulide shows good permeability through the intestinal mucosa. Model fitting on the data corrected for dilution yielded a permeability value  $P$  that was not statistically different from the one reported above, this indicating that, in our situation, experimental data variability was more important than the theoretical error associated

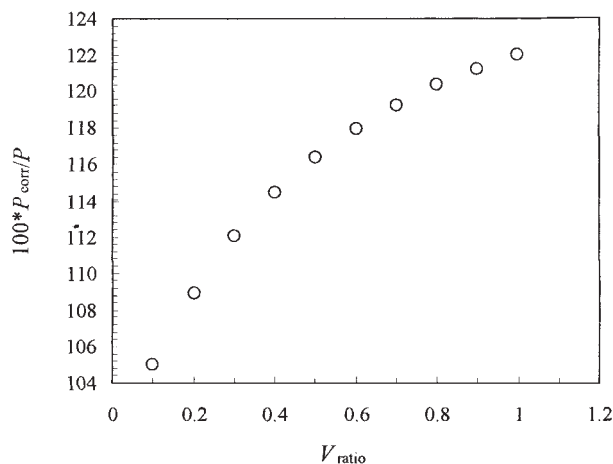


**Figure 8.**  $P_{\text{corr}}/P$  ratio variation as a function of  $V_{\text{ratio}}$  (ratio between sampled and receiver volume).

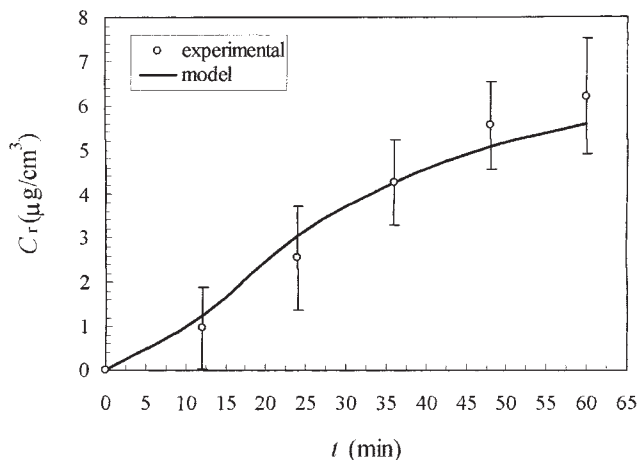


**Figure 9.** Model best fitting (solid line; eqs. 2–11) on the experimental data (circles; vertical bars indicate datum standard error).

with the use of eq. 16. Consequently, as data variability is much higher when working with living tissues, it could be reasonably expected that our warning became relevant dealing with permeation experiments involving more reproducible synthetic membranes.

Finally, it was interesting noticing that by means of our experimental finding (namely  $P$ ,  $k_d$ , and nimesulide solubility) it would have been possible to try an *in vitro/in vivo* correlation resorting to the theory developed by Oh<sup>44</sup> and Amidon.<sup>5</sup> Indeed, assuming a fixed value for the mean residence time in the intestinal lumen and knowing particle mean density, the dimensionless numbers  $Do$  (dose number),  $Dn$  (dissolution number), and  $An$  (absorption number) could have been evaluated for the activated system. These dimensionless numbers, ruling the fraction of dose absorbed, could have helped in trying an *in vitro/in vivo* correlation.

## CONCLUSIONS

Absorption experiments through everted rat intestine showed that ethanol–triacetin–nimesulide solution improved nimesulide bioavailability as it zeroed all the wettability problems connected with this drug. Moreover, we found that the activated system (PVP–nimesulide) was able to further increase nimesulide bioavailability as it overcame both nimesulide wettability and solubility problems. Interestingly, the activated system performance was even better than that of nimesulide solution, this being also due to the

experimental conditions adopted. Indeed, the hydrodynamic conditions and the presence of intestinal villi faced on the donor environment, gave rise to the formation of a thin layer surrounding the intestinal wall. In this layer, nimesulide concentration was higher than that in the bulk. The use of an *ad hoc* developed mathematical model allowed to estimate that this surplus concentration had to be equal to 30% of the bulk concentration.

Moreover, the developed mathematical model, allowing the determination of the Nimesulide permeability (or apparent diffusion coefficient), confirmed the fact that this drug shows a good permeability through the intestinal mucosa. The use of this model also allowed to conclude that an *a posteriori* data correction for dilution can reflect in a not negligible error on the drug diffusion coefficient (or permeability) estimation. Nevertheless, due to *in vivo* data variability, this error can be much more important when dealing with more reproducible synthetic membranes.

As the developed mathematical model was able to well fit the experimental release curves, we could be sure that the principal physical phenomena occurring during the release process were properly taken into account. In other words, nimesulide absorption through intestinal wall was ruled by passive diffusion and drug release from polymeric particles could be described by a proper dissolution constant.

## ACKNOWLEDGMENTS

The authors would like to thank the Centro servizi di Ateneo, Settore Stabulario e Sperimentazione animale of the Trieste University for the useful support provided and Italo Colombo, Lorenzo Magarotto, and David Ceschia for helpful discussion.

## REFERENCES

1. Waterbeemd van de H. 2000. Intestinal permeability: Prediction from theory. In: Dressman JB, Lennernäs H, editors. Oral drug absorption, prediction and assessment. New York: Marcel Dekker, pp 31–50.
2. Yu LX, Gatlin L, Amidon GL. 2000. Predicting oral drug absorption. In: Amidon GL, Lee PI, Topp EM, editors. Transport processes in pharmaceutical systems. New York: Marcel Dekker, pp 377–409.
3. Grassi M, Coceani N, Magarotto L. 2002. Modelling partitioning of sparingly soluble drugs in a two-phase liquid system. *Int J Pharm* 239:157–169.
4. Pharmacos 4, Eudralex collection, medicinal products for human use: Guidelines, volume 3C, p 234 (internet site: <http://pharmacos.eudra.org/F2/eudralex/vol-3/home.htm>).
5. Amidon GL, Lennernäs H, Shah VP, Crison JR. 1995. A theoretical basis for a biopharmaceutic drug classification: The correlation of *in vitro* drug product dissolution and *in vivo* bioavailability. *Pharm Res* 12:413–420.
6. Charman SA, Charman WN, Rogge MC, Wilson TD, Dutko FJ, Pouton CW. 1992. Self-emulsifying drug delivery systems: Formulation and biopharmaceutic evaluation of an investigational lipophilic compound. *Pharm Res* 9:87–93.
7. Constantinides PP. 1995. Lipid microemulsions for improving drug dissolution and oral absorption: Physical and biopharmaceutical aspects. *Pharm Res* 12:1561–1572.
8. Gasco MR. 1997. Microemulsions in the pharmaceutical field: Perspectives and applications. In: Solans C, Kunieda H, editors. Industrial applications of microemulsions. New York: Marcel Dekker; pp 97–122.
9. Pouton CW. Formulation of self-emulsifying drug delivery systems. *Adv Drug Del Rev* 25:47–58.
10. Kumar P, Mittal LK. 1999. Handbook of microemulsion science and technology. New York: Marcel Dekker, pp 755–771.
11. Frömring KH, Szejtli J. 1994. Cyclodextrins in pharmacy. Boston: Kluwer Academic Publishers.
12. Grassi M, Colombo I, Lapasin R. 2000. Drug release from an ensemble of swellable crosslinked polymer particles. *J Controlled Release* 68:97–113.
13. Dobbetti L, Cadelli G, Furlani D, Zotti M, Ceschia D, Grassi M. 2001. Reliable experimental setup for the drug release from a polymeric powder loaded by means of co-grinding. *Proc 28th Int Symp Controlled Release Bioact Mater* pp 728–729.
14. Buckton G, Beezer AE. 1992. The relationship between particle size and solubility. *Int J Pharm* 82:R7–R10.
15. Florence AT, Attwood D. 1987. Physicochemical principles of pharmacy. London: MacMillan Education LTD, Chapter V.
16. Adamson AW, Gast AP. 1997. Physical chemistry of surfaces. New York: Wiley Interscience, Chapt X.
17. Carli F, Colombo I. 1988. Physical state of drug loaded into silica gel carriers. *Acta Pharm Jugosl* 38:361–371.
18. Grassi M, Cadelli G. 2001. Theoretical considerations on the *in vivo* intestinal permeability determination by means of the single pass and recirculating techniques. *Int J Pharm* 229:95–105.
19. Fagerholm U, Lennernäs H. 1995. Experimental estimation of the effective unstirred water layer



- thickness in the human jejunum, and its importance in oral drug absorption. *Eur J Pharm Sci* 3:247–253.
20. Fagerholm U, Johansson M, Lennernäs H. 1996. Comparison between permeability coefficients in rat and human jejunum. *Pharm Res* 13:1336–1342.
  21. Lennernäs H, Ahrensted Ö, Ungell A-L. 1994. Intestinal drug absorption during induced net water absorption in man: A mechanistic study using antipyrine, atenolol and enalaprilat. *Br J Clin Pharmacol* 37:589–596.
  22. Nilsson D, Fagerholm U, Johansson M, Lennernäs H. 1994. The influence of net water absorption on the permeability of antipyrine and levodopa in the human jejunum. *Pharm Res* 11:1514–1545.
  23. Fagerholm U, Borgström L, Ahrensted Ö, Lennernäs H. 1995. The lack of effect of induced net fluid absorption on the in vivo permeability of terbutaline in the human jejunum. *J Drug Targeting* 3: 191–200.
  24. Uhing MR, Kimura RE. 1995. Active transport of 3-O-methyl-glucose by the small intestine in chronically catheterized rats. *J Clin Invest* 95:2799–2805.
  25. Palm K, Stenberg P, Luthman K, Artursson P. 1997. Polar molecular surface properties predict the intestinal absorption of drugs in humans. *Pharm Res* 14:568–571.
  26. Breitzkreutz J. 1998. Prediction of intestinal drug absorption properties by three-dimensional solubility parameters. *Pharm Res* 15:1370–1375.
  27. Grassi M, Coceani N, Cadelli G, Esposito P. 1999. Permeazione di acyclovir attraverso la mucosa intestinale di ratto: Esperimenti in vitro e modellazione matematica. *Bollettino Chimico Farmaceutico* 138:121–128.
  28. Wilson TH, Wiseman G. 1954. The use of sacs of everted small intestine for the study of the transference of substances from the mucosal to the serosal surface. *J Physiol* 123:116–123.
  29. Balimane PV, Chong S, Morrison RA. 2000. Current methodologies used for evaluation of intestinal permeability and absorption. *J Pharm Toxicol Methods* 44:301–312.
  30. Turner RH, Mehta CS, Benet LZ. 1970. Apparent directional permeability coefficients for drug ions: In vitro intestinal perfusion studies. *J Pharm Sci* 59:590–595.
  31. Meriani F, Coceani N, Sirotti C, Voinovich D, Grassi M. 2003. Characterization of a quaternary liquid system improving the bioavailability of poorly water soluble drugs. *J Colloid Interface Sci* 263:590–596.
  32. Davis R, Brogden RN. 1994. Nimesulide. An update of its pharmacodynamic and pharmacokinetic properties, and therapeutic efficacy. *Drugs* 48:431–454.
  33. Cignarella G, Vianello P, Berti F, Rossoni G. 1996. Synthesis and pharmacological evaluation of derivatives structurally related to nimesulide. *Eur J Med Chem* 31:359–364.
  34. Schilling RJ, Mira AK. 1990. Intestinal mucosal transport of insulin. *Int J Pharm* 62:53–64.
  35. Farraj NF, Davis SS, Parr GD, Stevens HNE. 1988. Absorption of progadibe from aqueous solutions in a modified recirculating rat intestinal perfusion system. *Int J Pharm* 43:93–100.
  36. Lindahl A, Krondahl E, Grudén AC, Ungell AL, Lennernäs H. 1997. Is the jejunal permeability in rats age-dependent? *Pharm Res* 14:1278–1281.
  37. Burgio N, Iasonna A, Magini M, Martelli S, Padella F. 1991. Mechanical alloying of the Fe–Zr system. Correlation between input energy and end products. *Il Nuovo Cimento* 13D:459–476.
  38. Theeuwes F, Hussain A, Higuchi T. 1974. Quantitative analytical method for the determination of drugs dispersed in polymers using DSC. *J Pharm Sci* 63:427–429.
  39. Meriani F. 2003. Valutazione ex vivo dell'assorbimento orale di nimesulide. Ph.D. thesis. University of Trieste, Department of Materials Engineering Science.
  40. Brun M, Lallemand A, Quinson JF, Eyraud C. 1973. Changement d'état liquide-solide dans les milieux poreux. *J Chimie Phys* 70:979–989.
  41. Patankar SV. 1980. Numerical heat transfer and fluid flow. New York: Hemisphere Publishing Corporation.
  42. Press WH, Teukolsky SA, Vetterling WT, Flannery BP. 1992. Numerical recipes in FORTRAN: The art of scientific computing. New York: Cambridge University Press, Chap 16.
  43. Flynn GL, Yalkowsky SH, Roseman TJ. 1974. Mass transport phenomena and models: Theoretical concepts. *J Pharm Sci* 63:479–510.
  44. Oh DM, Curl RL, Amidon GL. 1993. Estimation the fraction dose absorbed from suspensions of poorly soluble compounds in humans: A mathematical model. *Pharm Res* 10:264–270.